

## *Ab initio* study of the surface and interfacial properties of a layered MgO/NiO film

M. D. Towler

*Theoretical Chemistry Group, Department of Inorganic, Physical and Materials Chemistry, University of Torino,  
via P. Giuria 5, I-10125, Torino, Italy*

N. M. Harrison

*Daresbury Laboratory, Council for the Central Laboratory of the Research Councils, Daresbury, Warrington WA4 4AD, United Kingdom*

M. I. McCarthy

*Pacific Northwest Laboratory, MSK1-90, Richland, Washington 99352*

(Received 21 February 1995)

The equilibrium surface geometries of MgO and NiO, and the surface/interface geometry of layered composite thin films of these two oxides, are computed from first-principles periodic calculations within the unrestricted Hartree-Fock approximation. Calculated binding-energy shifts of the Ni  $2p$  core levels caused by geometric perturbations in the layered films are of the correct order of magnitude to account for published x-ray photoelectron spectroscopy results. Recent spectroscopic data may thus be interpreted in terms of an ioniclike model with modest surface relaxation.

### INTRODUCTION

A knowledge of the electronic structure and atomic geometry of oxide surfaces is essential to an understanding of many aspects of solid-state chemistry, particularly the study of catalytic processes and the way in which surfaces interact with adsorbed molecules and supported metals. Quantitative experimental data remain relatively scarce, despite significant advances in surface-sensitive analytic techniques, and there is a clear incentive for the use of theoretical methods to characterize surface properties of oxides at the atomic level. The use of *ab initio* theory is especially important since semiempirical techniques generally contain phenomenological parameters that may be inaccurate or simply inapplicable in complex cases like polar or adsorbate-covered surfaces.

This paper has two aims. The first is to report Hartree-Fock-level calculations of selected electronic and geometrical properties of composite-oxide thin films constructed of layers of MgO and NiO, which have recently been prepared.<sup>1</sup> The second is to interpret certain anomalous results of x-ray photoelectron spectra in these systems. In order to quantify the accuracy of the calculations, some surface properties of the pure oxides MgO and NiO are also examined.

#### Oxide thin films

Experimental techniques pioneered over the last few years by Goodman and co-workers have allowed the preparation of ultrathin metal-oxide films of only a few well-characterized monolayers on a metal substrate [see, e.g., Refs. 1–4]. The preparation and characterization of these essentially two-dimensional materials are currently topics of great interest both experimentally and theoretically. In catalysis, for example, it has been suggested that the structural and electronic properties of the substrate can influence the reactivity of the oxide overlayers

significantly, leading to potentially new catalytic mechanisms.<sup>5</sup> There is also a practical advantage to studying insulating materials in the form of supported thin films. Often the interpretation of spectroscopies which use electrons or ions as probes, such as x-ray photoelectron spectroscopy, is suspect in insulators because of strong perturbations resulting from photoemission-induced buildup of charge in the surface region (surface-charging effects). Thin films of the type synthesized by Goodman and co-workers appear to be amenable to study through such techniques because the excess charge is quenched by electrons tunneling from the metal substrate.

Recent progress by the Goodman group has allowed the synthesis of *composite* thin films on metal substrates, in which the oxide film is built from layers of different kinds of oxides. In this paper we shall be concerned principally with the layered MgO-NiO film grown on molybdenum reported in Ref. 1. We begin by noting the observed spectroscopic characteristics of this system. After deposition of an even layer of NiO on the metal surface, the results of ion-scattering spectroscopy (ISS) and low-energy electron diffraction (LEED) were used to show that layers of MgO could be grown epitaxially and evenly on the NiO, with virtually complete coverage occurring after deposition of only two monolayers. The question of whether the films were made up of distinct layers of NiO and MgO, or whether some interdiffusion took place, was addressed with electron-energy-loss spectroscopy (EELS). All the peaks in the EELS spectrum were assigned to transitions characteristic of single-oxide films, and no transitions involving electron transfer between the two oxides or interface states were observed. A final interesting effect was discovered through an x-ray photoelectron spectroscopy (XPS) determination of the core-level binding energies. As the thickness of the MgO overlayer was increased, the binding energies of the Ni  $2p$ , Mg  $2p$ , and O  $1s$  levels were found to undergo a substantial increase relative to the stationary  $3d$  level of the

Mo substrate, which was used as a reference. The explanation for this effect proposed by Burke and Goodman involved a mechanism requiring electron transfer from the MgO layer to the NiO. The calculations reported in this paper do not support this suggestion. We propose that the effect could be simply a consequence of changes in the surface geometry of the film upon deposition of the MgO overlayer.

In order to place the theoretical calculations in context, we first review some simple physical considerations relating to XPS and the physical reasons for core-level binding-energy shifts in insulators. The interpretation of Hartree-Fock eigenvalues as approximate experimental binding energies, and the nature of surface geometry changes in the rocksalt structure oxides NiO and MgO, are also briefly discussed.

#### X-ray photoelectron spectroscopy (XPS)

XPS (Ref. 6) involves the penetration of the solid surface by a photon of energy  $h\nu$ , which is absorbed by an electron with a binding energy  $E$  below the vacuum level. The electron is then ejected from the solid with a kinetic energy  $h\nu - E$ . The energy distribution of the electrons emitted from the surface records the spectrum of energy differences between the ground state of the sample and the numerous final states. These may be interpreted as one-electron binding energies. Since the zero of energy refers to the energy of an electron in a state of rest at an infinite distance from the solid, the energy to take the electron through the surface, or work function, is in principle included in the definition of the binding energy. Since ejected photoelectrons only have a relatively small energy-dependent mean free path in solids before being inelastically scattered, XPS probes layers only within about 10–50 Å of the surface.

The measurement of core-level binding-energy shifts via XPS is a valuable and widely used diagnostic tool in surface analysis (see the recent review by Egelhoff<sup>7</sup>). It is particularly important for determining the oxidation state of surface species. In general, anything which produces a sufficiently large change in the electrostatic potential experienced by a core electron at a particular site will produce a measurable shift in its binding energy. A useful, though not unique, classification of these changes is as *initial-state* and *final-state* contributions. The potential felt by a core electron at an atomic site, and hence its *initial-state* binding energy, is related to the charge density of all the other electrons in the system and the arrangement of ions in the lattice surrounding the site. Local-charge-density variations due to chemical effects or external fields, and changes in the Madelung potential at the site caused by lattice relaxation or proximity to a surface, will induce shifts in the binding energies. These can, in principle, be treated within the Hartree-Fock approximation.

*Final-state* effects arise as a consequence of the photoionization process. In the XPS final state, the electrons remaining at the atomic site after photoejection, together with those of neighboring ions, undergo a dielectric response to the sudden appearance of a positive core

hole. The energy liberated in this relaxation process can be transferred directly to the outgoing photoelectron. This process is inherently dependent on the time it takes the electron to escape from the solid. In the *adiabatic approximation* used in some theoretical XPS studies,<sup>6</sup> the emission of the photoelectron is assumed to be a slow process and the ion is therefore allowed to reach a stable final-state equilibrium configuration. In reality the photoionization process is rapid, and a more usual and apparently valid assumption is the *sudden approximation* in which the perturbation is switched on very rapidly. This leads to the presence of small satellite features in the XPS spectrum which are caused by excited final-state configurations. To a first approximation, all such final-state effects will produce similar binding-energy shifts at different atomic sites. If we consider only *relative* shifts and not absolute values of binding energies, the complex final-state effects are minimized. It should be noted that the magnitude of final-state effects depends to a certain extent on the polarizability of the atoms close to the site in question;<sup>8</sup> therefore in insulators one might expect to find significant changes in the magnitude of final-state effects for atoms either at a surface or at an interface with a metal.

#### Hartree-Fock eigenvalues

It is necessary to assess the accuracy of comparing Hartree-Fock one-electron eigenvalues with energies associated with photoelectron spectra. The definition of the Hartree-Fock eigenvalue using Koopmans' theorem<sup>9</sup> may be interpreted to first order as a one-electron binding energy. This implies that the initial-state eigenvalue exactly equals the difference between final and initial Hartree-Fock total energies of the system. In practice this approximation has been shown to be reasonable due to a cancellation of errors associated with ignoring both relaxation and correlation effects, which are opposite in sign, with typical magnitudes of around 1–2 eV.<sup>7</sup> Higher-order corrections such as relativistic and spin-orbit effects are ignored in our treatment.

#### Surface geometry

The (100) face of rocksalt-structure oxides like MgO and NiO is nonpolar and the most stable truncation of the bulk. The unrelaxed structure of this surface and a typical relaxed geometry are shown in Fig. 1. The structural perturbation at the surface is small and

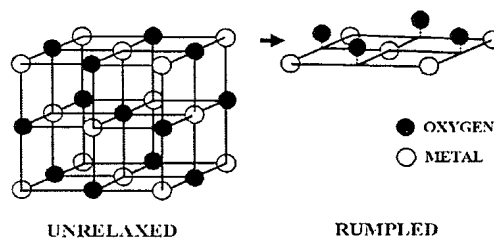


FIG. 1. Simple bulk termination of the MgO(100) surface and its most commonly predicted form of surface rumpling.

TABLE I. Experimental determinations and theoretical calculations of the surface geometry of MgO(100). The different sets of data for the shell model calculations refer to calculations using different interionic potential models. Rumpling and relaxation are defined in the text.

Reference	Technique	Relaxation (%)	Rumpling (%)
10	LEED	0 to -3	0 to +5
11	RHEED		+6
12	LEED	0±0.75	2±2
13	LEED	0 to +2.5	
14	RHEED	0 to +3	
15	ICISS	-15±3	0.3±0.9
16	LEED	1±2	5±2.5
17	shell model	0	+9
		0	+7
		0	+5
18	shell model	0	+3
		-2	+2
19	shell model	+1	+11
20	shell model	+0.6	+2.4
21	<i>ab initio</i> HF (CRYSTAL)		
	two-plane slab	+0.3	+1.0
	three-plane slab	0.0	+0.9
22	tight-binding model	-1.4±1.4	+2.4±1.4

difficult to determine in practice, but most experiments and calculations predict a small amount of relaxation and a nonzero rumple at the (100) surface in both MgO and NiO. Reported values from the literature are shown in Tables I and II. The figures given for relaxation and rumpling are defined in terms of the anion and cation displacements,  $x^+$  and  $x^-$ , from their unrelaxed positions as a percentage of the bulk interlayer spacing. Relaxation is given by  $\frac{1}{2}(x^+ + x^-)$  and rumpling by  $(x^- - x^+)$ .

There is considerable scatter in the reported experimental geometries. This is not unusual in studies of oxide surfaces, and there appear to be a number of reasons for such large uncertainties, among which differences in sample preparation and conditions are probably the most important. The use of approximate model theories used to interpret the results of experiments such as low-energy electron diffraction (LEED) may also be relevant in some cases.

Table II shows that ionic model calculations using the shell model<sup>27</sup> to represent ionic polarization give rather variable results, with reported rumplings in the outer layer of MgO between +2% and +11% of the interlayer spacing. Such calculations take into account short-range overlap forces, the long-range Coulomb interaction, and, in an approximate way, the most important aspects of the displacement-induced deformation of the charge density. In the shell model, the ions are approximated by a massive core linked to a massless shell by a harmonic spring constant  $k$ . The shell has a charge  $Y$  and the effective polarizability of an ion in the rocksalt structure is then  $Y^2/(k+S)$ , where  $S$  is the force between the ions due to the short-range potential. These shell model parameters have reasonably well-defined physical meanings and can generally be related to the elastic and dielectric constants of the crystal. Nevertheless, considerable care is needed in choosing them if accurate surface geometries are to be obtained, since the size and direction of rumpling in such

calculations is almost entirely attributable to the values chosen for the shell model parameters. In binary ionic crystals the surface ion having the greater polarizability tends to relax outwards relative to the other. Unfortunately, it is not always the case that potential parameters derived to reproduce bulk properties are applicable at the surface. Positive shell charges, for example, which sometimes emerge from bulk parameter-fitting procedures, produce the opposite sign of rumpling to negative shell charges. Such problems have been extensively discussed by Martin and Bilz,<sup>18</sup> and by de Wette, Kress, and Schröder.<sup>20</sup> They address the effect of including more physically realistic surface effects, such as changes in polarizability at the surface, quadrupole contributions, and overlap charge adjustments, in ionic model calculations.

#### THEORETICAL METHOD

To study the surface and interfacial properties of layered-oxide films, Hartree-Fock calculations were performed on model slabs that were infinitely periodic in two dimensions and consisted of a stack of up to seven atomic layers parallel to the exposed surface. Such structures bypass the unphysical approximations (related to the definition of the electrostatic boundary conditions) inherent in cluster calculations, which are frequently used to model surfaces. Both individual slabs of MgO and NiO and composite layered structures were considered.

TABLE II. Experimental determinations and theoretical calculations of the surface geometry of NiO (100).

Reference	Method	Relaxation (%)	Rumpling (%)
23	LEED	-2	0
24	LEED	0 to -3	-5 to +5
25	LEED	0 to -3	0 to -3
26	shell model	-0.7	-1.3

In order to create a model that would not generate long-range fields, it was necessary to build the composite systems from symmetrical slabs of the form MgO/NiO/MgO (where the number of layers in these systems will be denoted using a notation such as 2/3/2). This, of course, implies the neglect of the Mo substrate upon which the NiO film is grown, a feature of our calculations which may be justified as follows: (1) The MgO surface dipole will lead to an image potential<sup>28,29</sup> in the metal, that is, charge density will be shifted around near the NiO-Mo interface, creating an equal and opposite dipole to prevent the existence of a long-range electric field in the metal. To some extent this will mimic the presence of a second layer of MgO on the opposite face of the NiO film, as in our model. (2) NiO is an excellent insulator because of the Mott-Hubbard mechanism associated with the strong on-site Coulomb interaction in localized electron systems. This implies that electron transfer from the substrate (and between the two oxide films) is greatly inhibited. Note that this mechanism does not operate for a positively charged NiO film, and so surface-charging effects associated with XPS can be quenched by electron transfer from the metal. Furthermore, the original experimental data did not depend significantly on the thickness of the NiO film. It will be shown that it is not necessary to invoke the metal substrate to explain the spectroscopic observations.

The calculations were performed using the CRYSTAL program, a well-established package that has been used to study a wide range of crystalline materials.<sup>30,31</sup> This code employs a localized atomic-orbital basis set derived from Gaussian-type functions to construct Bloch functions, which are the basis in which the solid-state band-structure problem is solved. Recent modifications to the code<sup>32</sup> were used to perform open-shell calculations within the unrestricted Hartree-Fock formalism. There have been several previous studies of MgO surfaces using the CRYSTAL program, including treatments of the (001) surface,<sup>21</sup> the (110) surface,<sup>33</sup> and (100) surface-adsorbate interactions.<sup>34,35</sup> Problems relevant to the present work addressed in the first two of these studies were the reliability of the thin-film model for the study of surface properties, and the utility of basis sets optimized in studies of bulk properties for atoms at the surface. It was shown that if the repeat unit parallel to the desired crystal face corresponds to a relatively stable structure, then convergence of surface properties dependent on the total energy occurs very quickly with increasing slab thickness [ $\sim 2-3$  layers for MgO(100)]. As might be expected, the error associated with using the same basis set for inequivalent (surface and bulk) atoms was found to be negligible.

Reproduction of the bulk properties of magnetic insulators such as NiO using the methods of one-electron band theory has been a traditionally difficult theoretical problem. This is because the occupation of *localized* electron levels in these materials has an enormous effect on the energies of the unoccupied levels, producing a gap in the one-electron band spectrum. This feature is not reproduced in methods using a local approximation to the exchange, such as the local-spin-density approxima-

tion. It has been shown by us in previous work<sup>36,37,51</sup> that in Hartree-Fock (HF) theory the strong on-site Coulomb interactions responsible for the wide-band-gap insulating nature of these materials are correctly treated, which resolves the apparent conflict between band theory and experiment. At present, therefore, methods based on the Hartree-Fock approximation appear to be a useful starting point for the study of the ground state of magnetic insulators.

The Ni and O all-electron Gaussian atomic-orbital basis sets used in this work were the same as those used in our previous studies of bulk NiO (see, e.g., Ref. 37), while the Mg basis set was taken from Ref. 38. *3d* polarization functions were used in the Mg basis. Computational tolerances, which control the accuracy with which the Coulomb and exchange series are evaluated,<sup>31</sup> were set at the high level of ( $10^{-6}$ ,  $10^{-5}$ ,  $10^{-6}$ ,  $10^{-7}$ ,  $10^{-14}$ ) for all calculations.

Analytic gradients are not yet available within the CRYSTAL code, and thus all geometry optimizations were done numerically using repeated line searches. The equilibrium geometry of all ions in three- and five-layer slabs of MgO and NiO, together with the composite systems 1/3/1 and 2/3/2, were obtained in this way. Care was taken to carry out the calculations with the lattice parameters in the plane of the slab corresponding to the equilibrium structure of the bulk material at the same level of theory. This ensured that the surface would not distort in unphysical ways in response to an inappropriate lattice parameter.

Other studies<sup>39</sup> on the ZnO (10 $\bar{1}$ 0) surface have shown that the inclusion of *a posteriori* correlation corrections to the total energy in CRYSTAL appear to have little effect on computed surface geometries. Recent work by Causà and Zupan using a modified version of the CRYSTAL program<sup>40,41</sup> has shown that there is little consistent improvement to HF geometries using correlation corrections either at the Hartree-Fock, hybrid Hartree-Fock density-functional, or Kohn-Sham density-functional levels.

## RESULTS AND DISCUSSION

### Surface geometry of pure and composite films

The results of full surface geometry optimizations for each model slab are reported in Table III. The structure of three-layer MgO is similar to that found in an early CRYSTAL study<sup>21</sup> of the MgO surface, with minor differences due to the larger basis set and higher computational tolerances used in the present calculations. Our results are in qualitative agreement with most of the experimental data for MgO, with the anion displaced outwards relative to the Mg ion by around 1% of the interlayer spacing. The small positive rumple also found in NiO differs in sign from that obtained both in the shell model calculations of Tasker and Duffy,<sup>26</sup> and in the LEED study of Prutton *et al.*<sup>25</sup> In the composite systems, there is a rather large increase in total rumpling relative to the single oxide slabs when the geometry of the interface between the two oxides is included.

TABLE III. Results of surface geometry calculations in NiO, MgO, and MgO/NiO/MgO slabs. Increasing layer numbers refer to increasing depth below the surface. The figures for rumpling and relaxation are defined in the text, and are given both in Å and as a percentage of the bulk layer spacing.

System	Layer	Relaxation		Rumpling	
		(Å)	(%)	(Å)	(%)
(MgO) <sub>3</sub>	1	+0.008 08	+0.385	+0.024 18	+1.153
(MgO) <sub>5</sub>	1	+0.008 22	+0.392	+0.021 23	+1.012
	2	+0.000 42	+0.020	-0.000 95	-0.045
(NiO) <sub>3</sub>	1	+0.000 36	+0.017	+0.014 51	+0.681
(NiO) <sub>5</sub>	1	+0.001 90	+0.089	+0.013 57	+0.637
	2	+0.000 23	+0.011	+0.001 76	+0.083
1/3/1	1	+0.001 69	+0.798	+0.036 15	+1.707
	2	+0.019 51	+0.921	+0.007 99	+0.377
2/3/2	1	-0.013 34	-0.630	+0.022 58	+1.066
	2	+0.011 48	+0.542	+0.010 84	+0.512
	3	+0.020 48	+0.967	+0.009 41	+0.444

The total-energy data were also used to estimate surface formation energies, which are reported in Table IV, together with other values from the literature for comparison. Our data were calculated from

$$E_{\text{surface}} = \frac{(E_{\text{slab}} - NE_{\text{bulk}})}{2}, \quad (1)$$

where  $E_{\text{slab}}$  and  $E_{\text{bulk}}$  are the total energies of slab and single-cell bulk calculations, and  $N$  is the number of layers in the slab. Agreement with existing experimental and theoretical work shown in the table is good. The inclusion of more diffuse  $d$  valence functions in the basis set considerably reduces the calculated surface energies relative to those reported in the earlier CRYSTAL study of two- and three-layer MgO slabs.<sup>21</sup> For the nonpolar (100) surface, relaxation is small, and optimization of the surface geometry reduces the surface energy by only a small amount (less than 1%).

TABLE IV. Calculated total and surface energy per cell for various (001) slabs, compared with experimental and theoretical data.

System	Reference	No. of layers	Total energy (Hartree/cell)	Surface energy (Hartree/cell)
MgO (unrelaxed)	This work	3	-823.992 67	0.0247
MgO (relaxed)	This work	5	-1373.354 03	0.0247
NiO (unrelaxed)	This work	3	-823.993 11	0.0244
		5	-1373.356 32	0.0240
NiO (relaxed)	This work	3	-4745.373 81	0.0257
		5	-7908.990 47	0.0257
MgO	50 (experimental)			0.021-0.024
				0.023
MgO	26 (shell model)			0.022-0.024
				0.0287
MgO	49 (shell model)			
MgO	21 ( <i>ab initio</i> HF)	3	-823.926 18	0.0287

### Electronic structure

The results of a distributed multipole analysis of the electronic charge density in the surface region is given in Table V for various slabs. The ionic charges and the dipole and quadrupole moments that are not constrained by symmetry to be zero ( $z$  and  $2z^2 - x^2 - y^2$ , respectively) are reported. The definition of these quantities within the CRYSTAL program is discussed extensively in Ref. 42.

The analysis in Table V shows clearly that for all systems considered the form of the charge density in all non-surface layers is very similar to that in the bulk. The only change of any size occurs in the surface MgO layer, where a slight reduction in the ionicity of both components (of around  $0.04e-0.05e$ ) occurs. This change occurs independently of whether the surface MgO layer sits on bulk MgO or on NiO. Furthermore, there is no evidence of any large transfer of charge from MgO overlayers to underlying NiO, in contrast to the suggestion of Burke and Goodman.<sup>1</sup> The reported dipoles and quadrupoles show the extent to which the charge distributions of atoms in the surface region are deformed relative to bulk atoms. All surface dipoles are negative outward as a result of electron density spilling out into the vacuum. The surface quadrupoles in NiO are such that both the metal and oxygen ions are slightly expanded in a direction normal to the surface. By contrast, in MgO and the composite systems, the surface Mg ions are contracted in this direction. Smaller charge deformations also occur at the interface between MgO and NiO in the layered slabs.

An example of a charge-density difference map, which shows the difference between the charge density in the MgO/NiO/MgO 2/3/2 slab and that obtained from a superposition of spherical ionic densities, is given in Fig. 2. The scale is logarithmic so as to enhance detail near the surface; many of the features from Table V can be seen.

### Rumpling and XPS

In the study reported in Ref. 1, Burke and Goodman grew a NiO film of approximately 17 monolayers on a

TABLE V. Calculated electronic charges, dipoles, and quadrupoles for all symmetry-inequivalent ions in various model slabs relaxed to equilibrium geometry (a.u.). Bulk results are given for comparison.

System	Layer	Charge		Dipole		Quadrupole	
		oxygen	metal	oxygen	metal	oxygen	metal
(MgO) <sub>3</sub>	1	-1.813	+1.826	+0.0486	+0.0287	+0.1972	-0.1602
	2	-1.874	+1.849	0.0	0.0	+0.0458	+0.0728
(MgO) <sub>5</sub>	1	-1.813	+1.826	+0.0674	+0.0264	+0.2272	-0.1632
	2	-1.868	+1.856	+0.0167	+0.0156	+0.0291	+0.0338
	3	-1.863	+1.863	0.0	0.0	+0.0028	-0.0010
(NiO) <sub>3</sub>	1	-1.868	+1.880	+0.0850	+0.0263	+0.0627	+0.0199
	2	-1.889	+1.865	0.0	0.0	-0.0163	+0.0407
(NiO) <sub>5</sub>	1	-1.868	+1.880	+0.0855	+0.0263	+0.0636	+0.0127
	2	-1.883	+1.871	+0.0091	+0.0087	-0.0076	+0.0205
	3	-1.877	+1.878	0.0	0.0	-0.0024	-0.0010
1/3/1	1	-1.818	+1.835	+0.0156	+0.0461	+0.2575	-0.1767
	2	-1.885	+1.870	-0.0055	+0.0080	-0.0169	+0.0171
	3	-1.881	+1.876	0.0	0.0	+0.0204	+0.0086
2/3/2	1	-1.814	+1.830	+0.0686	+0.0281	+0.1808	-0.1647
	2	-1.873	+1.864	-0.0296	+0.0351	+0.0580	+0.0202
	3	-1.877	+1.874	-0.0265	+0.0011	-0.0359	+0.0030
	4	-1.882	+1.877	0.0	0.0	+0.0265	+0.0095
MgO	bulk	-1.863	+1.863	0.0	0.0	0.0	0.0
NiO	bulk	-1.877	+1.877	0.0	0.0	0.0	0.0

substrate of molybdenum metal. MgO films of varying thickness were then deposited on the oxide surface and XPS spectra recorded as a function of coverage. The Ni XPS spectrum was by far the most well-characterized experimentally, since the local environment of Mg and O ions changes a great deal as MgO is grown from fractions of a monolayer to multilayers. As the thickness of the MgO film was increased from zero to around seven layers, an increase in the binding energy of the Ni  $2p_{3/2}$  level of roughly 1 eV was observed. An examination of the published spectrum<sup>1</sup> reveals that around half of the apparent shift appears to develop after deposition of the first MgO monolayer. However, the precise functional form of the shift with coverage is presumably subject to some degree of uncertainty as changes in *shape* of the peak as a function of coverage may occur, and the number of MgO monolayers is not precisely determined. It is perhaps simpler to say merely that there is an increase in the binding energy of the Ni core levels after depositing MgO on the NiO surface.

The explanation given for the Ni shift was as follows.<sup>1</sup> If significant charge transfer across the interface from MgO to NiO occurs, the Fermi level of the NiO will be raised. However, at equilibrium, the chemical potential of the electrons in the metal must be the same as those in the oxide layer; the NiO Fermi level must therefore be pinned to that of the molybdenum substrate, implying, since the Mo  $3d_{5/2}$  line remains unchanged with differing MgO coverage, a consequent shift to higher binding energies of the Ni core levels. The results of our calculations shown in Table V imply that such a charge transfer does not take place.

The work of Duffy, Hoare, and Tasker<sup>43</sup> has shown that in ionic crystals, where long-range electrostatic fields can be maintained, the effect of the surface double layer is

important for accurate computations of vacancy formation energies. These arguments may be used to construct an alternative explanation of Burke and Goodman's XPS results, by examining the effect of changes in surface geometry on the XPS data. The calculated relaxations and rumplings are small, but are sufficient to produce significant changes in the electrostatic potential inside the slab. This can be demonstrated as follows.<sup>44</sup> When rumpling occurs at a surface, a lattice dipole  $\mu_l$  is formed. Furthermore, if the atoms are polarizable, the electric field at the surface leads to induced polarization dipoles  $\mu_p$  at each atom, giving a total surface dipole per unit area,  $\mu$ :

$$\mu = \frac{(\mu_l + \mu_p)}{A}, \quad (2)$$

where  $A$  is the area of the unit cell. The potential  $V$  due to the dipole  $\mu$  at some point in the bulk is  $|\mu|/(z^2 + r^2)^{3/2}$ , where  $z$  represents the depth of the point below the surface, and  $r$  the distance from the point parallel to the surface. Integration over the whole surface gives a potential  $V$  at this point of

$$V = 2\pi|\mu| \int_0^\infty \frac{zr}{(z^2 + r^2)^{3/2}} dr, \quad (3)$$

and hence

$$V = 2\pi|\mu|. \quad (4)$$

$V$  is therefore independent of the depth below the surface. Surface dipoles caused by reconstruction of atoms in the surface layer thus give rise to a constant potential in the interior of the sample, which may be important in calculations of core-level binding-energy shifts. One might think of the physical basis of this effect in XPS as follows.

When an ejected photoelectron travels from inside the sample through a negative-outward electrostatic dipole barrier at the surface, the electron will be retarded and consequently emerge with a lower kinetic energy. This is equivalent to a greater measured binding energy. Hence any effect which changes the magnitude of the surface dipole will affect the observed XPS spectrum.

The important point in the case of the layered oxide system is that, according to our calculations, the total rumpling and the resultant surface dipole increase when MgO is deposited on the surface (Table III). The effect of

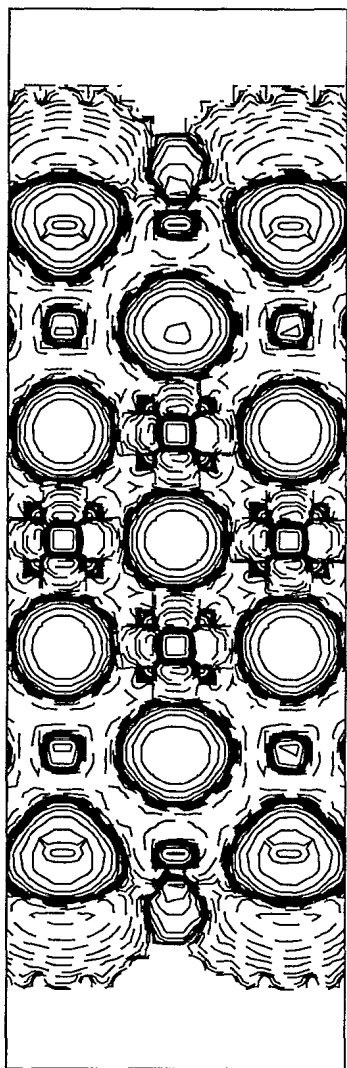


FIG. 2. Charge-density difference map of MgO/NiO/MgO 2/3/2 slab relaxed to equilibrium geometry. The map refers to the difference between the charge density from the periodic calculation and that of a superposition of spherical ionic densities. The plane shown is that through the ion centers and perpendicular to the [100] direction in the conventional unit cell. The large roughly spherical ions are oxygen ions, the aspherical ion in the central three layers is Ni, and the smaller ion in the outer two layers is Mg. Solid, dashed, and dot-dashed lines refer to positive, negative, and zero values, respectively. The absolute scale is logarithmic from  $1 \times 10^{-5}$  to 2.0 with three lines per power of 10, with an additional zero contour.

this on the Hartree-Fock Ni  $2p_z$  eigenvalues (at the  $\Gamma$  point) of the Ni ions in the middle three layers is shown in Fig. 3. It is apparent that moving from the bare nickel oxide surface to two overlayers of MgO gives a binding-energy increase in the Ni core levels of around 0.2–0.3 eV. This is roughly half the shift observed in the XPS spectrum for similar MgO coverages. This difference in rumpling might be accentuated in the real system due to the very slight discrepancy in the lattice constants of the two oxides, which is ignored in our treatment, and the presence of surface disorder. A comparison with calculations where the surface is merely a truncation of the bulk geometry is shown on the same plot. In Fig. 4, a similar plot on the same scale is given which shows the effect of simple relaxation (without rumpling) of the outer surface over a range of 4% of the bulk lattice spacing, which is greater than that actually observed. Since no change in surface dipole is involved in this case, there is little effect on the eigenvalue spectrum.

It is important to note that core-level shifts of this type should be detectable with overlayer films no more than a few monolayers thick, since it is *changes* in the surface double layer that appear to produce large chemical shifts. For relatively thick films the surface geometry should be independent of the number of layers. A further practical point is that substrate core levels (of Ni, in this case) can only be detected with XPS for relatively low MgO coverages.

In real systems, surface defects and disorder will affect the surface double layer. Shell model calculations<sup>45</sup> have suggested that nonplanar surfaces of MgO tend to be

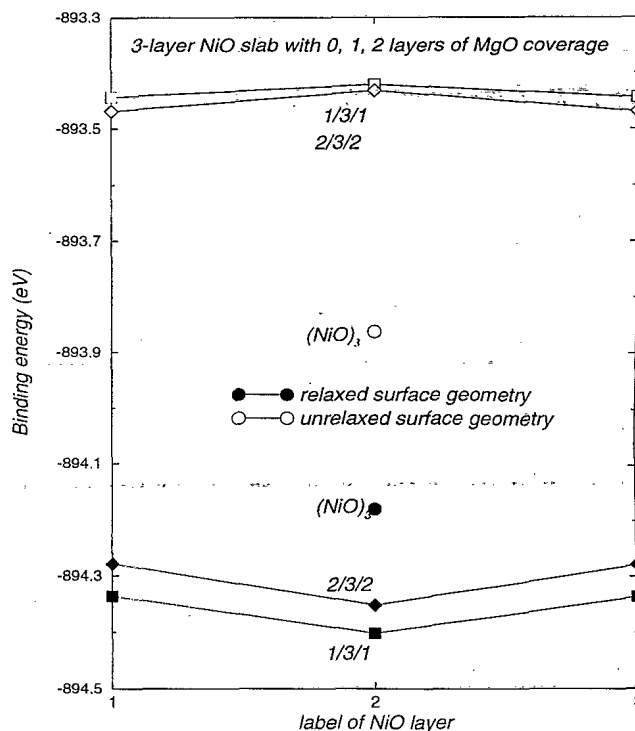


FIG. 3. Calculated Hartree-Fock eigenvalues at the  $\Gamma$  point for the Ni  $2p_z$  levels of the central three Ni layers, as a function of MgO coverage. Results for relaxed (filled points) and unrelaxed (unfilled points) surface geometries are compared.

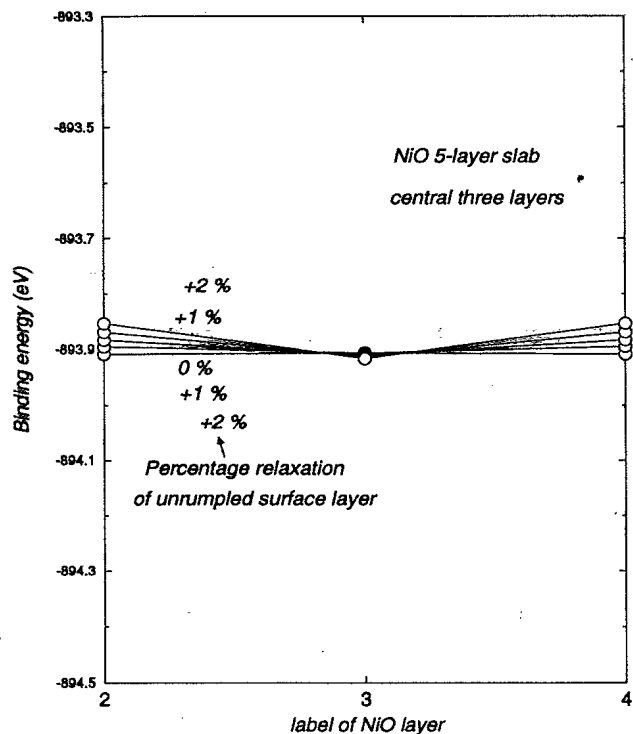


FIG. 4. Calculated Hartree-Fock eigenvalues for the Ni  $2p_z$  levels in the five-layer NiO slab, for differing amounts of surface relaxation. No rumpling of the surface was carried out. The energy scale is as in Fig. 3.

highly distorted. Compared with a calculated relaxation at a perfect (100) surface of less than 3% of the lattice spacing, ledge or step sites were found to be distorted by up to 15%, cavity sites by up to 14%, and corner sites by up to 38%, or about 0.8 Å. It can be surmised that such large distortions might be responsible for a proportion of the observed shifts.

#### Surface core-level shifts (SCLS)

Shifts in core-level binding energies for ions in the outermost layers relative to those of bulk ions are also of interest. Such surface core-level shifts are more difficult to compute accurately within the Hartree-Fock approximation because the final-state contribution is expected to be different at sites in the surface layer compared to other layers. However, the initial-state contribution to the SCLS depends partly on changes in the local charge distribution and partly on the difference in the Madelung potential at the surface site. The surface Madelung potential has been examined by a number of investigators;<sup>46-48</sup> its *magnitude* in the surface layer is found to be smaller than in the bulk by about 4% for the rocksalt structure. Hence electrons at surface cation sites are more deeply bound and electrons at surface anion sites less deeply bound than in the bulk. The calculated potential in the layer next to the surface is found to be almost indistinguishable from that in deeper layers.

In Figs. 5 and 6, calculated O  $1s$  and Ni  $2p_z$  Hartree-Fock eigenvalues as a function of atomic layer are reported for several different model slabs. The opposite sign of

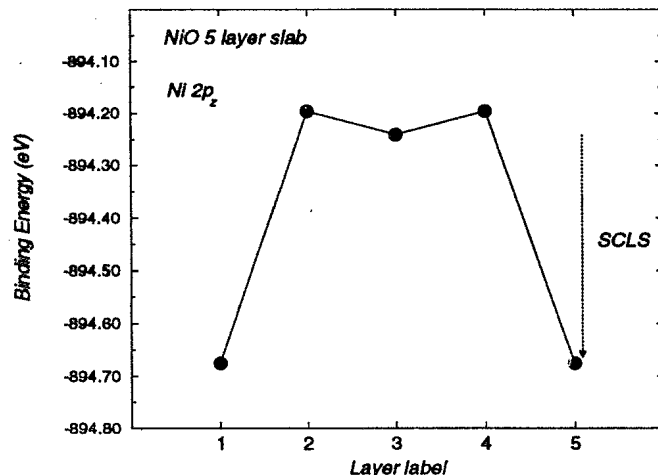


FIG. 5. Calculated Ni  $2p_z$  Hartree-Fock eigenvalues in the five-layer NiO slab.

the Madelung potential at anion and cation sites is reflected in the direction of the surface eigenvalue shifts, but the opposite shifts are not equal in magnitude. This is presumably due to local-charge-density effects; a decrease in ionicity of the surface atoms, for example, will tend to decrease the shifts due solely to the Madelung potential. Table V shows that a redistribution of charge occurs at the surface, consistent with a decrease in ionicity of both components.

Surface core-level shifts in metals are often interpreted in terms of the narrowing of the valence-band width of atoms at the surface due to their reduced coordination, with consequent redistribution of charge.<sup>7</sup> It is interesting to compare this picture with that for the insulator MgO. The density of states of the oxygen valence levels for surface and bulk atoms is shown in Fig. 7, where it is seen that there is little appreciable difference in the bandwidth in the two cases, as might be expected for a highly ionic material.

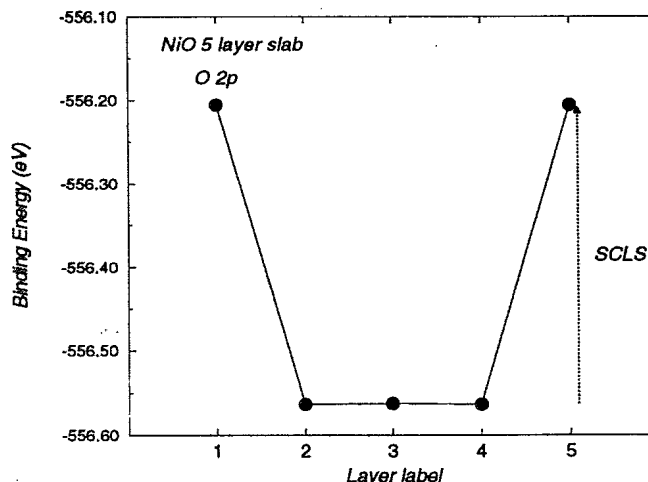


FIG. 6. Calculated O  $1s$  Hartree-Fock eigenvalues in the five-layer NiO slab.



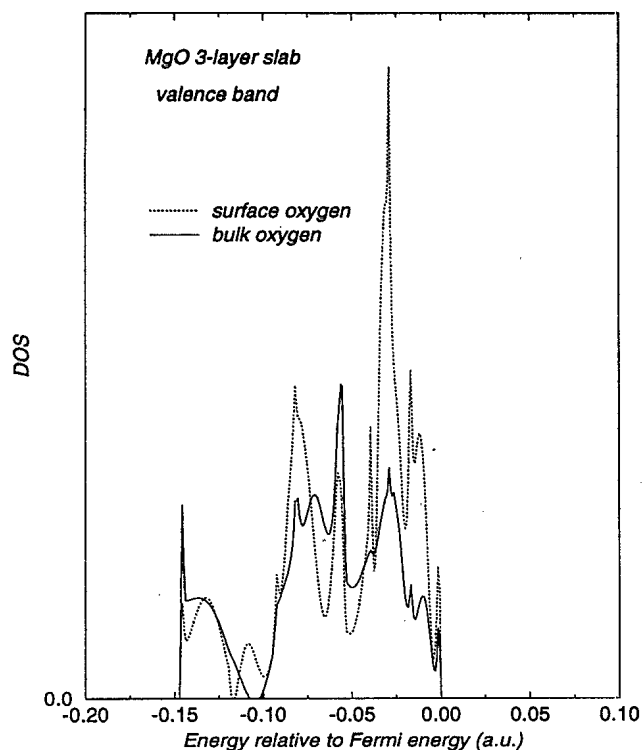


FIG. 7. O 2p and O 2s projected density of states for valence bands of ions in the bulk and surface layers of a MgO three-layer slab.

### CONCLUSIONS

The equilibrium surface geometries of three- and five-layer MgO and NiO, and the surface/interface geometry of the layered oxides MgO/NiO/MgO 1/3/1 and 2/3/2, have been calculated from first principles within the Hartree-Fock approximation. Agreement with available experimental data is reasonably good, and clearly the method is an attractive one for the study of surface struc-

ture. Binding-energy shifts based on Hartree-Fock eigenvalues for the Ni 2p levels in the layered oxides were also calculated. Shifts due to changes in the surface and interface geometries of the composite slabs relative to the pure NiO surface were shown to be of the correct order of magnitude and direction to account for the XPS results of Burke and Goodman.<sup>1</sup> The shifts are therefore consistent with an ionic-like model with modest surface relaxations. Our results do not support the hypothesis of MgO to NiO charge transfer suggested by these authors to account for their spectra.

In conclusion, our calculations suggest that small surface geometry changes can have significant effects on the initial states of ions in oxide materials.

### ACKNOWLEDGMENTS

M.I.M. gratefully acknowledges support from the Division of Chemical Sciences of the Office of Basic Energy Sciences, U.S. Department of Energy, under Contract No. DE-AC06-76RLO-1830. M.D.T. wishes to thank the Northwest College and University Association for Science (WSU) for one month's support under Grant No. DE-FG06-89ER-75522 with the Department of Energy, and also the Commission of the European Communities for the award of a fellowship under the Human Capital and Mobility Programme (Contract No. ERBCH-BICT941605). We would also like to acknowledge computational resources provided by SERC Grants Nos. GR/H07160 and GR/J26243, and the Scientific Computing Staff of the Office of Energy Research, U.S. Department of Energy for a grant of computing time at the National Energy Research Supercomputing Center. The work was also partially supported by European Community HC&M Contract No. CHRX-CT93-0155. Pacific Northwest Laboratory is operated for the U.S. Department of Energy by Battelle Memorial Institute under Contract No. DE-AC06076RLO1830.

<sup>1</sup>M. L. Burke and D. W. Goodman, *Surf. Sci.* **311**, 17 (1994).

<sup>2</sup>M.-C. Wu, J. S. Corneille, J.-W. He, C. A. Estrada, and D. W. Goodman, *J. Vac. Sci. Technol. A* **10**, 467 (1992).

<sup>3</sup>C. M. Truong, M.-C. Wu, and D. W. Goodman, *J. Chem. Phys.* **97**, 9447 (1992).

<sup>4</sup>M.-C. Wu, C. M. Truong, and D. W. Goodman, *J. Phys. Chem.* **97**, 4182 (1993).

<sup>5</sup>D. G. Kinniburgh and M. L. Jackson, in *Adsorption of Inorganics at Solid-Liquid Interfaces*, edited by M. A. Anderson and A. J. Rubin (Ann Arbor Science, Ann Arbor, 1981).

<sup>6</sup>D. P. Woodruff and T. A. Delchar, *Modern Techniques of Surface Science* (Cambridge University Press, Cambridge, 1989).

<sup>7</sup>W. F. Egelhoff, *Surf. Sci. Rep.* **6**, 253 (1987).

<sup>8</sup>E. Rotenberg and M. A. Olmstead, *Phys. Rev. B* **46**, 12 884 (1992).

<sup>9</sup>T. C. Koopmans, *Physica* **1**, 104 (1933).

<sup>10</sup>C. G. Kinniburgh, *J. Phys. C* **9**, 2695 (1976).

<sup>11</sup>T. Gotoh, S. Murakimi, K. Kinoshita, and Y. Murata, *J. Phys. Soc. Jpn.* **50**, 2063 (1981).

<sup>12</sup>M. R. Welton-Cook and W. Berndt, *J. Phys. C* **15**, 5691

(1982).

<sup>13</sup>T. Urano, T. Kanaji, and M. Kaburagi, *Surf. Sci.* **134**, 109 (1983).

<sup>14</sup>P. A. Maksym, *Surf. Sci.* **149**, 157 (1985).

<sup>15</sup>H. Nakamatsu, A. Sudo, and S. Kawai, *Surf. Sci.* **194**, 265 (1988).

<sup>16</sup>D. L. Blanchard, D. L. Lessor, J. P. LaFemina, D. R. Baer, W. K. Ford, and T. Guo, *J. Vac. Sci. Technol. A* **9**, 1814 (1991).

<sup>17</sup>M. R. Welton-Cook and M. Prutton, *Surf. Sci.* **74**, 276 (1978).

<sup>18</sup>A. J. Martin and H. Bilz, *Phys. Rev. B* **19**, 6593 (1979).

<sup>19</sup>G. V. Lewis and C. R. A. Catlow, *J. Phys. C* **18**, 1149 (1985).

<sup>20</sup>F. W. de Wette, W. Kress, and U. Schröder, *Phys. Rev. B* **32**, 4143 (1985).

<sup>21</sup>M. Causà, R. Dovesi, C. Pisani, and C. Roetti, *Surf. Sci.* **175**, 551 (1986).

<sup>22</sup>J. P. LaFemina and C. B. Duke, *J. Vac. Sci. Technol. A* **9**, 1847 (1991).

<sup>23</sup>J. B. Marsh and H. E. Farnsworth, *Surf. Sci.* **1**, 3 (1964).

<sup>24</sup>C. G. Kinniburgh and J. A. Walker, *Surf. Sci.* **63**, 274 (1977).

- <sup>25</sup>M. Prutton, J. A. Walker, M. R. Welton-Cook, R. C. Felton, and J. M. Ramsey, *Surf. Sci.* **84**, 95 (1979).
- <sup>26</sup>P. W. Tasker and D. M. Duffy, *Surf. Sci.* **137**, 91 (1984).
- <sup>27</sup>B. G. Dick and A. W. Overhauser, *Phys. Rev.* **112**, 90 (1958).
- <sup>28</sup>A. M. Stoneham and P. W. Tasker, *J. Phys. C* **18**, L543 (1985).
- <sup>29</sup>D. M. Duffy, J. H. Harding, and A. M. Stoneham, *Philos. Mag. A* **67**, 865 (1993).
- <sup>30</sup>C. Pisani, R. Dovesi, and C. Roetti, *Hartree-Fock Ab Initio Treatment of Crystalline Systems*, Lecture Notes in Chemistry Vol. 48 (Springer, Berlin, 1988).
- <sup>31</sup>R. Dovesi, V. R. Saunders, and C. Roetti, *CRYSTAL 92 User Documentation* (Università di Torino, Torino, 1992).
- <sup>32</sup>E. Aprà, Ph.D. thesis, Università di Torino, Italy, 1993.
- <sup>33</sup>M. Causà, R. Dovesi, E. Kotomin, and C. Pisani, *J. Phys. C* **20**, 4983 (1987).
- <sup>34</sup>M. I. McCarthy, A. C. Hess, N. M. Harrison, and V. R. Saunders, *J. Chem. Phys.* **98**, 6387 (1993).
- <sup>35</sup>C. A. Scamehorn, A. C. Hess, and M. I. McCarthy, *J. Chem. Phys.* **99**, 2786 (1993).
- <sup>36</sup>M. D. Towler, Ph.D. thesis, University of Bristol, U.K., 1994.
- <sup>37</sup>M. D. Towler, N. L. Allan, N. M. Harrison, V. R. Saunders, W. C. Mackrodt, and E. Aprà, *Phys. Rev. B* **50**, 5041 (1994).
- <sup>38</sup>R. Dovesi, C. Roetti, C. Freyria-Fava, E. Aprà, V. R. Saunders, and N. M. Harrison, *Philos. Trans. R. Soc. London Ser. A* **341**, 203 (1992).
- <sup>39</sup>J. E. Jaffe, N. M. Harrison, and A. C. Hess, *Phys. Rev. B* **49**, 11 153 (1994).
- <sup>40</sup>M. Causà and A. Zupan, *Chem. Phys. Lett.* **220**, 145 (1994).
- <sup>41</sup>M. Causà and A. Zupan, *Int. J. Quantum Chem.* (to be published).
- <sup>42</sup>V. R. Saunders, C. Freyria-Fava, R. Dovesi, L. Salasco, and C. Roetti, *Mol. Phys.* **77**, 629 (1992).
- <sup>43</sup>D. M. Duffy, J. P. Hoare, and P. W. Tasker, *J. Phys. C* **17**, L195 (1984).
- <sup>44</sup>W. C. Mackrodt, *J. Chem. Soc. Faraday Trans. 2* **85**, 541 (1989).
- <sup>45</sup>E. A. Colbourn and W. C. Mackrodt, *Solid State Ionics* **8**, 221 (1983).
- <sup>46</sup>R. R. Slater, *Surf. Sci.* **23**, 403 (1970).
- <sup>47</sup>D. E. Parry, *Surf. Sci.* **49**, 433 (1975).
- <sup>48</sup>R. E. Watson, J. W. Davenport, M. L. Perlman, and T. K. Sham, *Phys. Rev. B* **24**, 1791 (1981).
- <sup>49</sup>E. A. Colbourn, W. C. Mackrodt, and P. W. Tasker, *J. Mater. Sci.* **18**, 1917 (1983).
- <sup>50</sup>P. W. Tasker, *J. Phys. C* **12**, 4977 (1979).
- <sup>51</sup>W. C. Mackrodt, N. M. Harrison, V. R. Saunders, N. L. Allan, M. D. Towler, E. Aprà, and R. Dovesi, *Philos. Mag. A* **68**, 653 (1993).